European Journal of Pharmaceutics and Biopharmaceutics 120 (2017) 34–42

Contents lists available at ScienceDirect

European Journal of Pharmaceutics and Biopharmaceutics

journal homepage: www.elsevier.com/locate/ejpb

Research paper

Novel concentrated water-in-oil emulsions based on a non-ionic silicone surfactant: Appealing application properties and tuneable viscoelasticity

Lisa Binder[a], Johannes Jatschka[a], Dieter Baurecht[b], Michael Wirth[a], Claudia Valenta[a,c,*]

[a] University of Vienna, Department of Pharmaceutical Technology and Biopharmaceutics, Faculty of Life Sciences, Althanstraße 14, 1090 Vienna, Austria
[b] University of Vienna, Department of Physical Chemistry, Faculty of Chemistry, Währingerstraße 42, 1090 Vienna, Austria
[c] University of Vienna, Research Platform 'Characterisation of Drug Delivery Systems on Skin and Investigation of Involved Mechanisms', Althanstraße 14, 1090 Vienna, Austria

ARTICLE INFO

Keywords:
Water-in-oil emulsion
Silicone surfactant
Skin-friendly
Skin permeation
ATR-FTIR
Tape stripping

ABSTRACT

Silicone excipients are non-irritating ingredients that are extensively used in topical formulations. In the present study, innovative water-in-oil emulsions with a high water content stabilised by a non-ionic silicone surfactant were developed. Effects of formulation composition on its properties and stability were investigated. It was possible to prepare highly stable emulsions with a water volume fraction of up to 80%. The emulsions exhibited desirable application properties such as non-sticky and cooling qualities. A dependency of the viscosity on the water fraction was found; this offers the opportunity to create emulsions with fine-tuned rheological properties.

Furthermore, it could be shown in skin studies that the *in vitro* release of a hydrophilic model drug is influenced by the configuration of the oil phase. The penetration of the silicone surfactant and the other deployed additives was monitored using combined tape stripping and ATR-FTIR experiments, revealing that the compounds remain in the superficial layers of the stratum corneum, thus minimising the risk for skin irritation.

1. Introduction

There is a wide range of scientific literature dealing with emulsion formulation and characterisation; however, the majority is focusing on oil-in-water (O/W) emulsions. In the field of water-in-oil (W/O) emulsions, wherein an aqueous phase is dispersed in an oil phase, the research seems to be much scarcer. One explanation for the limited number of studies might be that in the past, W/O emulsions were more difficult to prepare due to a lack of applicable surfactants, especially if aiming for high water content. Concerning the analysis of W/O systems, a dilution with water is not possible owing to the immiscible property of ambient oil phase and water. This represents a major challenge as many analytical techniques cannot be deployed.

Despite these difficulties, W/O emulsions offer distinct advantages for dermal application. When applied, a continuous film is formed immediately due to the direct contact of the external oil phase with the skin surface; this oil film helps maintaining the flexibility and hydration of the skin [1]. W/O emulsions offer the possibility to include a hydrophilic active pharmaceutical ingredient (API) within the inner water phase; thus, the API is protected against extrinsic impacts by the continuous oil film.

Silicone surfactants, based on a polysiloxane backbone composed of alternating silicon and oxygen atoms, are predestined for the stabilisation of W/O emulsions. The properties of the emulsifier can be adapted by modifying the functional groups attached to the siloxane polymer chain [2]. Using silicone surfactants, it is possible to stabilise a particular large portion of aqueous phase. The high water content facilitates the incorporation of a large proportion of water-soluble API; additionally, it imparts a sensation of coolness when applied.

Silicones have been used in personal care products over many decades; they can be considered safe for topical use as they are non-toxic and do not affect the microstructure of stratum corneum (SC) lipids [3]. A recent study found that despite their water-resistant properties, silicone excipients act non-occlusive [4]. Unlike other W/O surfactants, silicone emulsifiers do not need waxes for additional stabilisation; this makes the formulations more appealing for the user [1]. Consequently, W/O emulsions stabilised by silicone surfactants offer excellent properties for widespread cosmetic and pharmaceutical application.

The objective of this study was to develop and characterise new skin-friendly W/O emulsions with the non-ionic silicone surfactant Dow Corning® Emulsifier 10 as stabiliser. The influence of the formulation

Abbreviations: O/W, oil-in-water; W/O, water-in-oil; API, active pharmaceutical ingredient; SC, stratum corneum; ATR, attenuated total reflection; FTIR, Fourier transform infrared spectroscopy

* Corresponding author at: University of Vienna, Department of Pharmaceutical Technology and Biopharmaceutics, Faculty of Life Sciences, Althanstraße 14, 1090 Vienna, Austria.
E-mail address: claudia.valenta@univie.ac.at (C. Valenta).

http://dx.doi.org/10.1016/j.ejpb.2017.08.003
Received 4 July 2017; Received in revised form 8 August 2017; Accepted 10 August 2017
Available online 12 August 2017

composition on its properties and stability should be elucidated. To this end, oils with different polarities were chosen as constituents of the continuous phase. In order to assess the role of emulsifier concentration and water volume fraction, the emulsions were stabilised by 2–4% emulsifier at different water-to-oil ratio. The produced emulsions were characterised in terms of appearance, skin feel, rheological behaviour and stability.

Furthermore, it was of interest to investigate the performance of the emulsions in terms of dermal drug delivery. Novel W/O emulsions that are able to deliver APIs through the SC may serve as useful new dermal drug delivery option; previous carrier systems designed for incorporation of hydrophilic actives, such as liposomes, have drawbacks regarding their storage stability [5,6]. In this study, two different model drugs were incorporated into the developed emulsion systems and *in vitro* Franz-type diffusion cell experiments were carried out using porcine skin. In doing so, the effect of the oil component and formulation composition on the percutaneous permeation of the model drugs was investigated.

Besides the interaction of an incorporated API with the skin, the behaviour of the non-active ingredients of the formulation when applied onto skin should be considered as well. There have been some efforts to analyse the interaction of silicone components with the skin tissue [7,8]; however, the penetration behaviour of the silicone content is not yet fully elucidated. To determine the penetration depth of the silicone additive Emulsifier 10, *in vitro* skin studies were conducted using a combination of the tape stripping technique with ATR-FTIR (attenuated total reflection-Fourier transform infrared) spectroscopy. Thus, knowledge about the skin irritation potential of the silicone surfactant could be obtained as skin irritation is presumably linked to the spatial distribution of a surfactant in the SC [9]. Additionally, the penetration of the two deployed oils into the skin has been investigated.

2. Materials and methods

2.1. Materials

Dow Corning® Emulsifier 10, a silicone surfactant with a hydrophilic lipophilic balance (HLB) value of 2.2, was kindly donated by Biesterfeld Spezialchemie (Hamburg, Germany). Liquid paraffin, isopropyl myristate and sodium chloride were obtained from Herba Chemosan Apotheker-AG (Vienna, Austria). Bodipy 493/503 (4,4-difluoro-1,3,5,7,8-pentamethyl-4-bora-3a,4a-diaza-s-indacene) was purchased from Invitrogen (Eugene, OR, USA) while fluorescein sodium salt, curcumin and Atto 594 were purchased from Sigma-Aldrich (St. Louis, MO, USA).

Abdominal porcine skin was bought from a local butcher, pig ears were obtained from a local abattoir (EU-Schlachthof Gantner, Hollabrunn, Austria) and stored at −24 °C up to a maximum of 6 months. Tesa film crystal clear polypropylene tape (product number 58247-00000, Hamburg, Germany) was used to remove the layers of the SC during tape stripping experiments.

2.2. Preliminary experiments and formulation development

To investigate the effect of chemical differences in the oil phase on emulsion formation and characteristics, two oils with different polarities were chosen for the preparation of the W/O emulsions; isopropyl myristate and liquid paraffin, with polarity indexes (mN/m) 24.2 and 38.3, respectively. In preliminary experiments, it was investigated whether it was possible to produce suitable and stable enough systems with both selected oils. Subsequently, the applicable ratio of ingredients was identified.

Taking into account the results of our preliminary investigations, six formulations were selected for further examination. The final emulsions were stabilised by 2–4% emulsifier at water-to-oil ratio of 20–80% and 18–37%; the composition of the selected emulsions is given in Table 1.

Table 1
Composition of the investigated W/O emulsions in% (w/w).

Emulsion	Excipients			
	Emulsifier 10	Liquid paraffin	Isopropyl myristate	Water phase[a]
PAR_2/18	2	18	–	80
PAR_4/36	4	36	–	60
IPM_2/18	2	–	18	80
IPM_2/28	2	–	28	70
IPM_3/27	3	–	27	70
IPM_3/37	3	–	37	60

[a] Composed of distilled water containing 1% (w/w) sodium chloride.

2.3. Emulsion preparation

The emulsions were prepared by first mixing Emulsifier 10 with the selected oil. Subsequently, the water phase, consisting of freshly distilled water and 1% sodium chloride for formulation stability, was added to the oil phase under moderate stirring (750 rpm). Specifically, the water had to be added slowly to the oil phase so that the emulsifier could thoroughly coat the water droplets. In a last step, the mixture was subjected to an ultraturrax (Omni 5000, Omni International, Kennesaw, USA) at 2500 rpm for 4 min to obtain the final W/O emulsion. The production process was consistently carried out at room temperature.

Additionally, emulsions with model drugs were produced; fluorescein sodium salt and curcumin were used as hydrophilic and hydrophobic model drugs, respectively. To this end, emulsions were loaded with either 0.1% (w/w) of fluorescein sodium salt or 3% (w/w) of curcumin by adding the drug in powder form to the water or oil phase before merging them.

2.4. Emulsion characterisation and stability monitoring

The produced emulsions were characterised immediately after preparation and monitored over an observation period of 20 weeks. In order to detect any instability such as creaming or phase separation, they were investigated for the presence of structures visible to the eye. Likewise, each sample was characterised regarding consistency and skin feeling.

The pH value of the emulsions was determined using a pH meter (Orion 420A, Bartelt, Austria) with an Orion ROSS micro pH electrode (8220BNWP). The rheological properties were likewise investigated in regular intervals over a period of 20 weeks with a cone-and-plate system. Optical light and fluorescence microscopy was employed to gain detailed insight into the structures of the formulations.

The developed emulsions were prepared and analysed in triplicate (n = 3); they were stored in sealed glass containers at 4 °C in a refrigerator.

2.5. Optical microscopy

Optical microscopy was applied to characterise the morphology of the emulsions and to observe structures in the micrometer size range. The examinations were carried out using an epifluorescence microscope (Zeiss Axio Observer.Z1 microscopy system, Carl Zeiss, Oberkochen, Germany) equipped with phase contrast and differential interference contrast (DIC). A small amount of each sample was placed on a microscopy slide, covered and observed immediately. Images were processed using AxioVision software Rel 4.8.2 (Carl Zeiss, Oberkochen, Germany).

Selected emulsions were investigated by fluorescence microscopy. Therefore, the fluorescent dyes Atto 594 and Bodipy were incorporated into the formulations as visual markers for either aqueous or oil phase. These fluorescent labels were chosen according to their excitation and emission maxima; besides optical considerations, the solubility in water

was of interest. Fluorescently labelled emulsions were prepared by adding the fluorescent dye to either oil or water phase prior uniting both phases. The hydrophilic Atto 594 (590 nm/≥615 nm) was incorporated into the water phase, whereas the lipophilic Bodipy (470 nm/525 nm) was employed to stain the oil phase. An overlay of the images provides information about the localisation of the two dyes and was thereby used to identify the continuous and dispersed phases.

2.6. Rheological characterisation

For all developed emulsions, continuous and oscillatory measurements were performed on a MCR Modular Compact Rheometer 302 (Anton Paar, Graz, Austria) with a thermostatic control system. The formulations were loaded into the device equipped with a cone-and-plate measuring system (diameter: 25 mm; cone angle: 2°). The temperature was maintained at 32 °C ± 0.2 °C throughout all measurements, simulating the skin surface temperature.

Flow curves were recorded for all formulations. To describe the flow behaviour of the emulsions, the dynamic viscosity η (in Pa s) was measured under shear stress. A controlled shear rate ranging from 1 to 100 s^{-1} and back from 100 to 1 s^{-1} was employed.

Furthermore, oscillatory shear experiments were performed to probe the viscoelasticity of the formulations. Thereby, the response of a sample which is exposed to sinusoidal stress is investigated. An amplitude sweep as a function of strain was conducted to identify the linear and nonlinear viscoelastic regions. Consequently, a fresh sample was loaded onto the rheometer and a frequency sweep test was performed in the frequency range of 1–40 Hz at the pre-selected shear strain. The storage modulus G′, loss modulus G″ and the loss factor tan δ were measured.

The rheological properties of the emulsions were observed immediately after preparation and monitored in regular intervals over a period of 20 weeks to determine the stability over time. All measurements were carried out in triplicate.

2.7. Solubility of curcumin in the acceptor medium

The saturation solubility of curcumin in the envisaged receptor medium, a mixture of ethanol: phosphate-buffered saline, pH 7.4 (50:50 v/v), was determined. To this end, an excess of the model drug was added to 1 ml of the medium and shaken for 24 h at room temperature. Afterwards, the dispersion was centrifuged at 5000 rpm for 10 min to separate undissolved drug. The supernatant was filtered (Ophthalsart 0.2 µm, Sartorius stedim Biotech GmbH, Göttingen, Germany) and the filtrate was analysed by absorbance spectroscopy at 422 nm.

Four individual experiments were performed (n = 4).

2.8. Skin permeation studies

In vitro skin permeation studies were conducted using Franz-type diffusion cells (Permegear, Hellertown, USA). For each formulation, at least ten replicate experiments were performed (n ≥ 10). Porcine skin was chosen as model system since it represents an acknowledged substitute for human skin [10,11].

Abdominal porcine skin was cut to a thickness of 700 µm with a dermatome (GB 228R, Aesculap, Center Valley, USA) and attached between the donor and receptor compartment of the diffusion cells having a diffusion area of 0.95 cm^2. Depending on the model drug, an appropriate receptor solution was selected. In case of fluorescein sodium, the receptor compartment was filled with 2 ml of phosphate-buffered saline, pH 7.4 (PBS). For the formulations with curcumin, the receptor solution consisted of a mixture of ethanol: PBS (50:50 v/v) to maintain sink conditions [12]. The cells were placed in a temperature controlled water bath at the skin temperature of 32 ± 0.2 °C and the receptor medium was stirred with magnetic bars. To ensure infinite dose conditions, 0.5 g of the formulation was applied to each skin sample. Subsequently, the donor chamber was occluded with Parafilm® to prevent evaporation. Samples were withdrawn at defined time intervals. In case of fluorescein sodium, the whole receptor solution was removed and replaced by fresh PBS; in case of curcumin, samples of 500 µl were withdrawn and immediately replaced by an equal volume of fresh receptor medium. Subsequently, the amount of model drug was analysed by fluorescence and absorbance spectroscopy.

2.9. Quantification of fluorescein sodium by fluorescence spectroscopy

The fluorescence of fluorescein sodium was measured using a fluorescence microplate reader (Tecan™ infinite 200, Tecan Ltd., Maennedorf, Switzerland) with an excitation wavelength of 485 nm and an emission wavelength of 535 nm. Calibration curves from standard solutions of fluorescein sodium in PBS (pH 7.4) ranging from 0.002 to 1.06 µg/ml for quantification were linear with a coefficient of determination of $R^2 = 0.9997$. Samples containing a higher content of the model drug were diluted; they were homogenised and centrifuged prior to analysis. From each solution, 100 µl were transferred into a 96-well plate in triplicate.

2.10. Quantification of curcumin by absorbance spectroscopy

For quantification of curcumin concentrations, sample absorbance was measured at 422 nm on a microplate reader (Tecan™ infinite 200, Tecan Ltd., Maennedorf, Switzerland). A similar approach like that of the quantification of fluorescein sodium was used. A standard curve, generated by dilution of a stock solution of curcumin in a mixture of ethanol: PBS (50:50 v/v), was used for quantification; standard solutions were ranging from 0.024 to 25.5 µg/ml with a coefficient of determination of $R^2 = 0.9999$. The samples were diluted and prepared as described above.

In the data analysis, the amount of receptor solution removed and the adequate dilution as a consequence of replacement with fresh solution were taken into account.

2.11. Combined ATR-FTIR and tape stripping experiments

The penetration of the emulsion components Emulsifier 10, liquid paraffin and isopropyl myristate into the SC was investigated by combined ATR-FTIR and tape stripping experiments according to a previously reported method by our working group [13]. Similar to the permeation studies described above, porcine skin was chosen as model for human skin.

On the day of the experiment, pig ears were defrosted and the full-thickness skin was removed from the cartilage with a scalpel. The skin was carefully freed from hair with scissors, cut into strips of 2 × 7.5 cm and fixed to pieces of Styrofoam with needles on the sides. The modified elasticity of skin removed from the cartilage and thereby formed wrinkles might lead to variabilities in the amount of removed skin [14,15]. Consequently, the tape stripping outcomes may be influenced in a negative way. Thus, the skin samples were carefully stretched prior fixation to minimise the occurrence of furrows.

Subsequently, 80 µl of the respective emulsion component were applied on the porcine ear skin sample and incubated for 2 h in a PBS-filled Petri dish in a water bath, maintaining the skin surface temperature of 32 ± 0.2 °C. After incubation, the samples were blotted dry with a soft tissue to remove all residuals of the applied substances. Sequentially, fifteen adhesive tape strips were placed on the skin sample and removed in a continuous movement, as uniformly as possible. ATR-FTIR spectra were recorded from the skin surface prior to the tape stripping procedure as well as after every tape stripping step. All experiments were performed at least in triplicate (n ≥ 3). In the exact same manner, skin samples were impregnated with 80 µl distilled water and stripped thereafter. These samples served as control to account for the intra-individual variability in SC composition.

Spectra were recorded using an ATR-FTIR spectrometer (Tensor 27, Bio-ATR I tool, Bruker Optics, Ettlingen, Germany) equipped with a liquid nitrogen cooled mercury cadmium telluride (MCT) detector. In the process, skin samples were placed on the ZnSe ATR crystal with the SC facing down. In order to obtain an adequate and constant contact between the probe and the crystal, samples were burdened with a weight of 100 g. Spectra were recorded at skin surface temperature of 32 °C. For each sample, 60 scans were collected in a double sided mode with a resolution of 4 cm^{-1} in the range of 4000–870 cm^{-1} using Blackman-Harris 3-term apodisation and a zero filling factor of 8.

Additionally, the pure emulsion components were applied directly on the ZnSe crystal and analysed separately. ATR-FTIR spectra were recorded under the same conditions as the incubated skin samples.

2.12. Infrared data analysis

The spectra collected were analysed using OPUS software version 5.5 (Bruker Optics, Ettlingen, Germany). Peak areas were calculated using OPUS integration mode B. A straight line is generated between the points of intersection of the measured absorbance and the two frequency limits defined; the area above this line is then integrated.

Spectra of the water incubated control samples were subtracted from the treated samples as described by Hoppel et al. [13]. Thus, the problem of overlapping signals of the applied substances with typical absorbance bands of the skin was avoided. In order to eliminate potential sources of error caused by variations in the overall absorbance of the spectra due to varying contact of the sample and the ATR surface, the amide II absorbance was used as an internal intensity standard since it is influenced by water to a lesser extent compared to the amide I band [16]. The frequency limits for integration were 1580–1487 cm^{-1} for the amide II absorbance. As the absorption coefficients of the characteristic absorption bands of the analysed components differ, spectra were normalised using the corresponding absorbances of the directly measured emulsion components as reference. The defined frequency limits for integration were 1272–1245 cm^{-1} and 1130–988 cm^{-1} for Emulsifier 10, 1478–1430 cm^{-1} and 1385–1363 cm^{-1} for liquid paraffin, as well as 1761–1718 cm^{-1} and 1124–1093 cm^{-1} for isopropyl myristate.

2.13. Protein quantification by NIR-densitometry

The corneocyte content of porcine SC removed with the individual adhesive films was quantified using the infrared densitometer SquameScan® 850A (Heiland Electronic GmbH, Wetzlar, Germany). The device determines the pseudo-absorption of the SC proteins on the tape strips at a wavelength of 850 nm. Since for the ATR-FTIR experiments tapes with a larger area than the standard adhesive tapes are required, these tapes had to be cut down to 4.0 cm^2 before inserting them into the sampling cassette with the adhesive side up. The device was calibrated by measuring the pseudo-absorption for a blank tape strip and correcting the pseudo-absorption of the sample strips against this value. The pseudo-absorption (A) value displayed in% can be converted into the mass of SC proteins (m) in $\mu g/cm^2$; this is done by employing the equation m = A/0.224 [17]. SC thickness was calculated by removing tape strips until the measured pseudo-absorption was below the detection limit of the densitometer [18]. The total SC thickness results from the sum of the calculated amounts of SC on all tapes. A mean SC thickness of porcine ear skin of 12.26 µm was determined in twelve parallel experiments (n = 12).

2.14. Statistical analysis

Statistical analysis was performed using Microsoft Excel 2010 (Microsoft Corporation, WA, USA) and GraphPad Prism 3.00 (GraphPad Software, CA, USA). Changes in the formulation properties were tested for statistical significance using Student's *t*-test. In case of repeated measurements, paired *t*-tests were carried out. Non-parametric data were analysed using the Mann-Whitney *U* test. A p value of < 0.05 was considered to indicate a statistical significance.

3. Results and discussion

3.1. Emulsion characterisation and physicochemical stability

Emulsions stabilised by the silicone surfactant Emulsifier 10 were prepared with varying composition. The main objectives were to produce pleasant and stable W/O emulsions and to assess the influence of different oil components on essential emulsion properties. It was possible to prepare silicone surfactant based W/O emulsions that initially were homogenous with both oils deployed. As a consequence of preliminary studies, the emulsifier content was kept low at a maximum of 4% and the fraction of the water and oil phase was varied between 60–80% and 18–37%, respectively. The applied emulsification method did not involve a heating step; therefore, it can be considered advantageous for the use of heat-sensitive substances.

In an initial visual inspection, no signs of creaming or sedimentation could be detected for any of the prepared formulations. While liquid paraffin gave creamy emulsions with a fluffy structure, the emulsions with isopropyl myristate overall showed a comparably higher fluidity and a milky appearance. The varying in the ratio of inner and outer phase seemed to have an impact on fluidity; this assumption was further investigated by rheological measurements. Texture analysis and sensory analysis revealed a pleasant, non-sticky skin feeling and no particular inherent odour of the product. When applied onto the skin, the formulation seemed to burst as the oil phase forms a continuous film and water evaporates. Thus, they had a pleasantly cooling effect on the skin and did not feel tacky because of the low oil content of the residual film. Especially the creamier emulsions revealed behaviour as described.

The morphology of the emulsions was visualised using optical microscopy. To avoid a change in the inner structure, the microscopic analysis was carried out without prior dilution of the samples. A homogenous structure with a dense network of small droplets could be observed for all prepared emulsions (Fig. 1). The size of the emulsion droplets was determined by microscopic examination. For emulsions prepared with liquid paraffin, it varied within a range of around 20 µm for occasionally observable large droplets down to few micrometres for the much higher share of small droplets (Fig. 1A and 1B). The emulsion IPM_2/18 (Fig. 1C) exhibited a similar microstructure compared to the corresponding formulation prepared with liquid paraffin (PAR_2/18). In case of the other emulsions prepared with isopropyl myristate, the structure appeared denser and the biggest droplets had a size of about 10 µm (Fig. 1D–F).

After the initial characterisation, the morphology of all produced formulations was monitored in regular intervals over a period of 20 weeks. Over the whole observation period, the emulsions remained macroscopically as well as microscopically stable with no observable changes in appearance and microstructure.

The internal structure of the formulations was further confirmed by fluorescence microscopy. A comparison of a fluorescence microscopic image with the corresponding phase contrast image of PAR_4/36 dyed with both fluorescent dyes is given in Fig. 2. The overlay fluorescence images showed evenly dispersed water droplets, dyed with Atto 594 (red colour), throughout the green fluorescent continuous oil phase. Depending on the formulation, a large number of incorporated air bubbles visible as uncoloured black spots was found. Conversely, although the emulsions contained a comparatively higher amount of dispersed inner phase than continuous phase, the amount of green dyed oil phase appeared higher in the microscopic images. Presumably, due to the fact that the dense network of small water droplets is enclosed by an oil and surfactant layer, the background appeared green as a whole. In order to check this assumption, further tests with the fluorescent

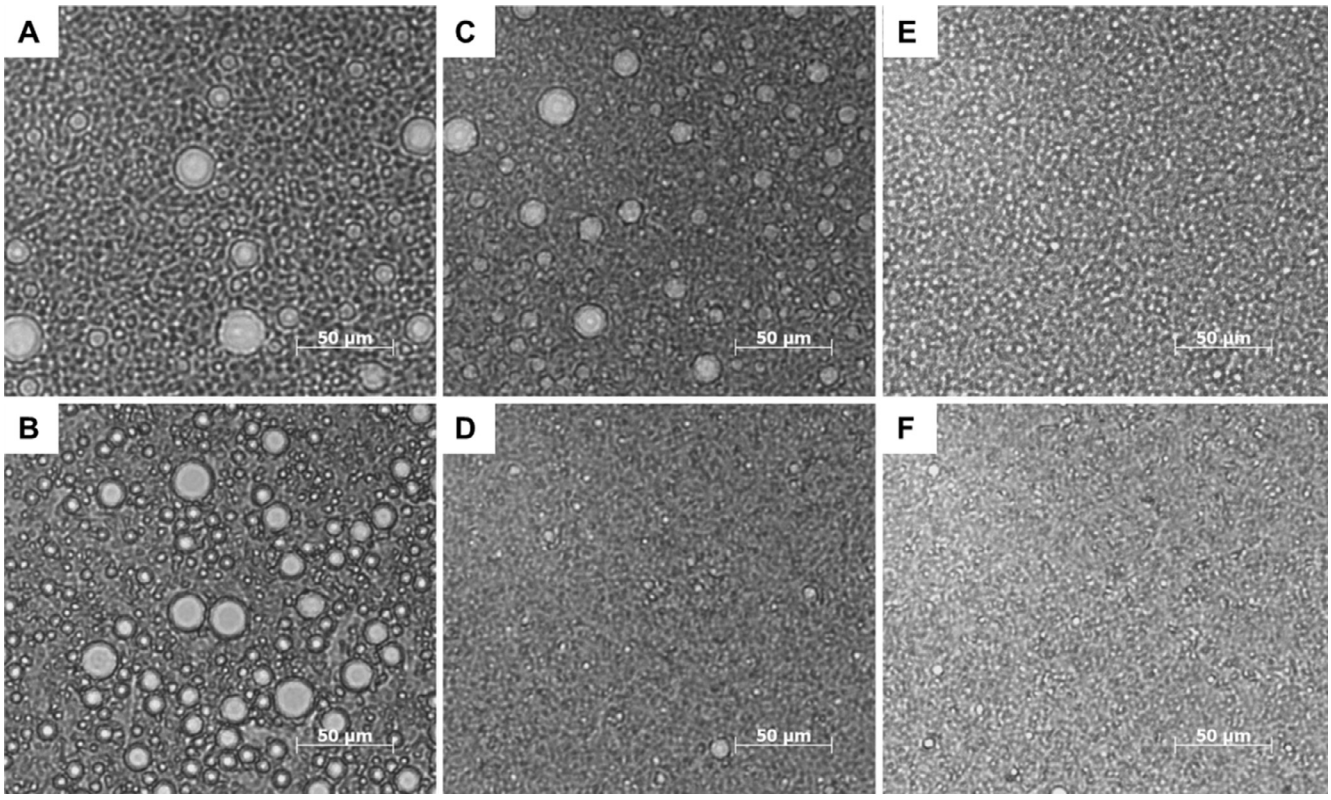

Fig. 1. Microscopic images of the prepared W/O emulsions inspected with a light microscope at 200-fold magnification: (A) PAR_2/18, (B) PAR_4/36, (C) IPM_2/18, (D) IPM_2/28, (E) IPM_3/27 and (F) IPM_3/37.

dyes were carried out. Looking at the green colour channel (Bodipy) separately, dark droplets could be distinguished in front of a green fluorescent background; these could be both water droplets and air bubbles. On the contrary, the analysis of the red coloured channel (Atto 594) reveals an entirely red coloured image; solely small black air bubbles could be observed. The findings endorse the theory that the water droplets are outshined by the surrounding oil phase when both fluorescent dyes are used.

The pH value was measured in regular intervals to detect destabilisation of the formulations induced by chemical degradation [19]. The pH values of the fresh emulsions were in the range of 4.47–5.45 for both oil phases (data not shown). The formulations with liquid paraffin showed a significant increase in pH during storage ($p = 0.02$ and $p = 0.03$ respectively). Except from IPM_3/37, all emulsions with isopropyl myristate showed unaltered pH values over the period of 20 weeks. In case of IPM_3/37, a significant decrease from 5.45 to 4.82 was observed after 20 weeks ($p = 0.02$). However, the overall pH suits the natural skin surface pH; therefore, the produced emulsions are convenient for dermal application [20].

3.2. Rheological measurements

Rheological measurements help to describe microstructural effects of emulsions; the flow properties depend on various factors like the chemical composition of each phase, relation of dispersed and continuous phase as well as the surfactant of the emulsion [21]. Therefore, a rheological characterisation has been undertaken to elucidate the impact of the used material and ratio of ingredients. As the water-to-oil

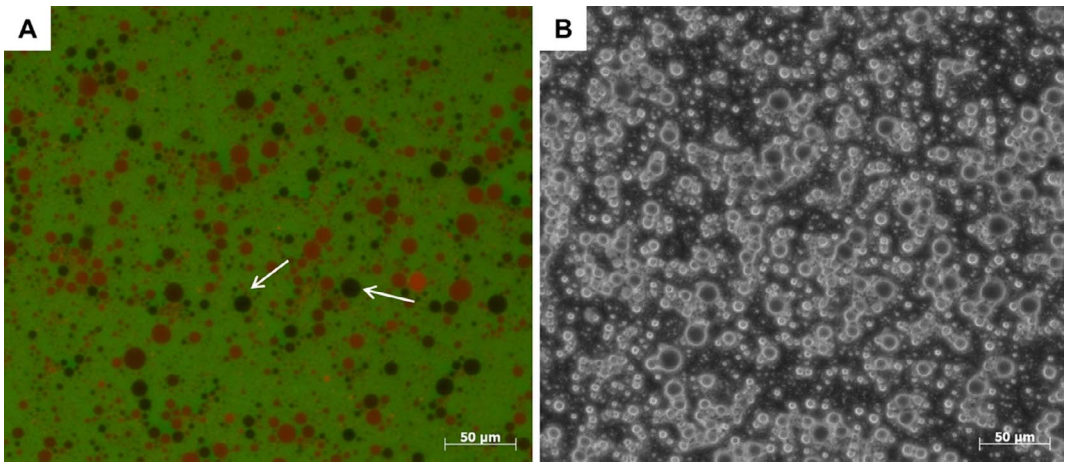

Fig. 2. Microscopic images of PAR_4/36 after incorporation of Bodipy and Atto 594 inspected at 200-fold magnification: (A) fluorescence microscopic image and (B) image obtained using phase contrast mode. Air bubbles are marked by white arrows.

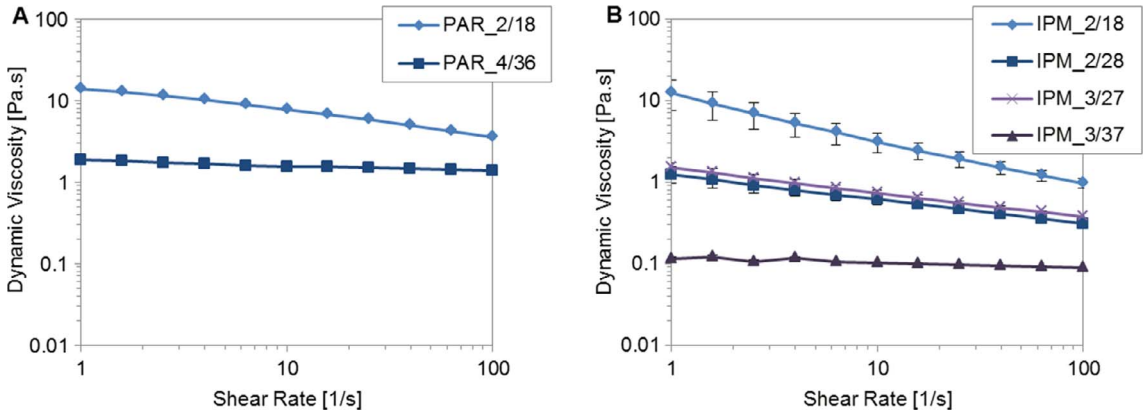

Fig. 3. Dynamic viscosity as a function of shear stress for (A) emulsions prepared with liquid paraffin and (B) emulsions prepared with isopropyl myristate as oil component. The depicted curves are means ± SD of three experiments (n = 3).

Table 2
Storage (G'), loss modulus (G″) and loss factor (tan δ) as determined in oscillatory measurements on fresh emulsions, compared at a frequency of 1 Hz. The depicted values are means ± SD of three experiments (n = 3).

Formulation	G′	G″	tan δ
PAR_2/18	22.60 ± 1.97	47.53 ± 0.81	2.11 ± 0.15
PAR_4/36	1.79 ± 0.54	8.62 ± 0.40	5.15 ± 1.7
IPM_2/18	205.70 ± 143.92	37.80 ± 11.57	0.26 ± 0.18
IPM_2/28	1.97 ± 0.58	2.32 ± 0.40	1.21 ± 0.16
IPM_3/27	4.15 ± 1.12	3.53 ± 0.51	0.87 ± 0.11
IPM_3/37	0.27 ± 0.00	0.43 ± 0.02	1.58 ± 0.07

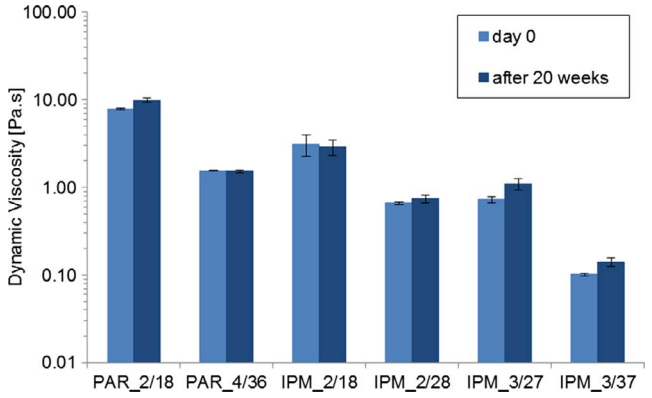

Fig. 4. Effect of storage on emulsion viscosity: Comparison of the dynamic viscosity at a shear rate of 10 s^{-1} at 32 °C. Values were determined on fresh emulsions and after 20 weeks of storage. Three experiments were performed for each formulation (n = 3).

ratio was varied just as the surfactant concentration, changes in flow behaviour for the different emulsions were anticipated.

Via flow curves, viscosity changes between shear rates of 1 and 100 s^{-1} were measured. Independent from the type of oil, all emulsions showed pseudoplastic flow. Interestingly, the dynamic viscosity of the investigated emulsions covered a wide range. Compared at a shear rate of 10 s^{-1}, the by far lowest value of 0.1 Pa s was found in IPM_3/37. While the formulation PAR_2/18 showed the highest viscosity of 7.78 Pa s, the corresponding emulsion prepared with isopropyl myristate as oil component was significantly less viscous (3.11 Pa s). As expected, these findings indicate a relation between the oil type used and the viscosity of the emulsions.

In Fig. 3, the dynamic viscosity is illustrated as a function of shear stress. As can be seen, the water content influenced the rheological behaviour of the emulsions. With increasing water volume fraction, the dynamic viscosity of the system increased. This was true for all emulsions independent of the oil type. Such characteristics could be explained by the increase of the droplet-droplet interactions as the packing of water droplets gets dense [22]. The dependence of the viscosity on the water content enables the possibility to modify the properties of the systems according to the water-to-oil ratio. In this manner, it is feasible to create silicone based W/O emulsions with a fine-tuned viscosity.

The flow curves of IPM_2/28 and IPM_3/27 displayed in Fig.3B facilitate a comparison of the effect of the concentration of the surfactant. The viscosity of the emulsion was comparable for both surfactant concentrations; it seemed to be independent of the percentage of surfactant.

The structure of the formulations was further characterised using a

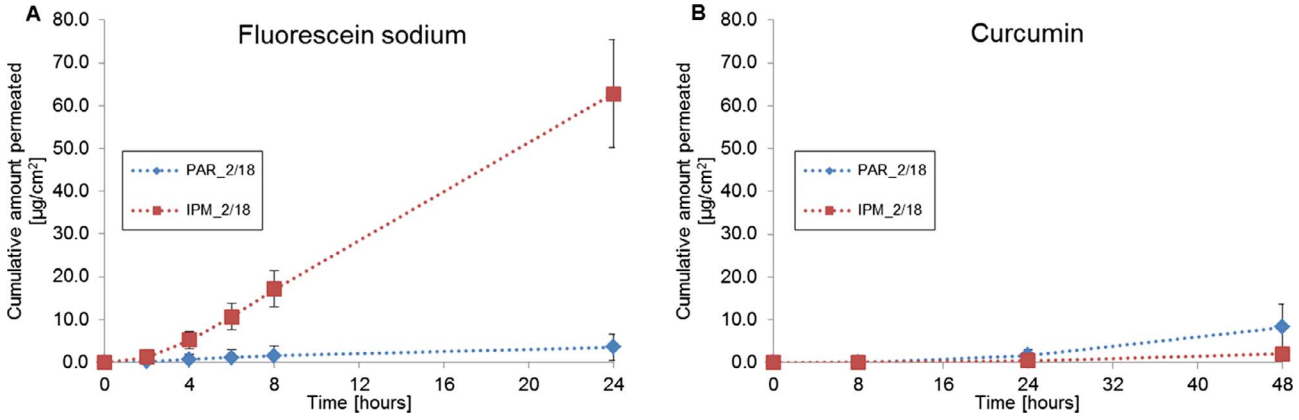

Fig. 5. Permeation profiles of (A) fluorescein sodium and (B) curcumin through abdominal pig skin from two W/O emulsions. Drug amounts were determined by fluorescence and absorbance spectroscopy respectively. The depicted curves are means ± SD of at least 10 experiments (n ≥ 10).

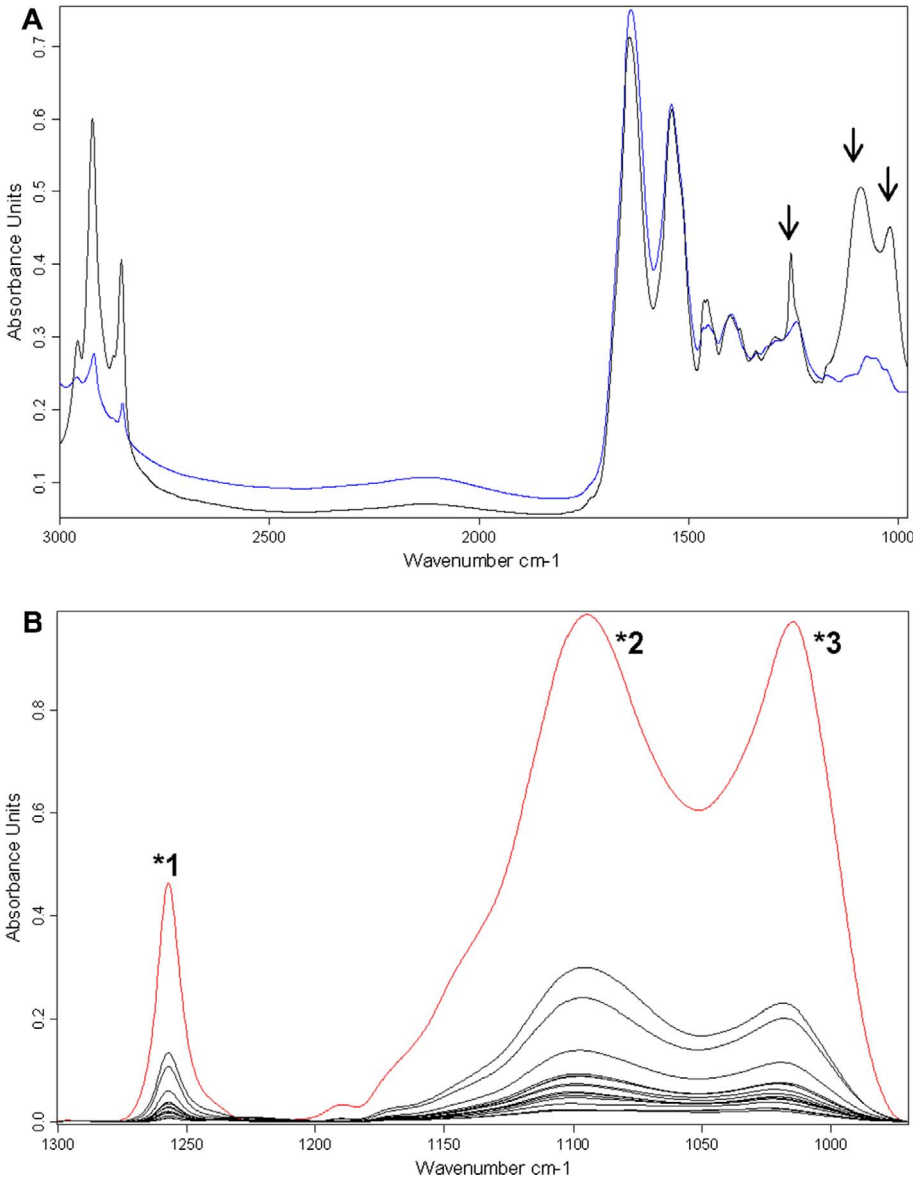

Fig. 6. (A) Representative ATR-FTIR spectra of porcine ear skin incubated with water (blue) and Emulsifier 10 (black). The arrows mark the characteristic absorption bands of Emulsifier 10 used for the calculation of the peak areas. (B) Difference spectra of Emulsifier 10 treated skin and water treated-skin from 15 tape-stripped layers (black) compared to the reference spectrum of Emulsifier 10 in direct contact with the ZnSe crystal (red); assignment of absorption bands to representative structure elements: (*1) symmetric deformation vibration of the CH_3 in the $Si{-}CH_3$ group at 1257 cm^{-1}, (*2) and (*3) asymmetric Si–O–Si stretching mode at 1094 cm^{-1} and 1014 cm^{-1}, respectively. (For interpretation of the references to colour in this figure legend, the reader is referred to the web version of this article.)

frequency sweep. This enables the determination of G′, G″ and tan δ using a constant shear stress and a variable frequency; hence, it provides more information about the interactions among droplets. The storage modulus G′ is a measure for the energy stored reversibly within in the system, characterising the elastic behaviour. The loss modulus G″ represents the dissipated and irreversibly lost energy, characterising the viscous behaviour. The loss factor, tan δ = G″/G′, describes the relation between the viscous and elastic portion of the sample [23,24].

Prior to the frequency sweep test, the linear viscoelastic range was detected by exerting an amplitude sweep and an appropriate shear strain was chosen. The mean G′, G″ and tan δ values at a frequency of 1 Hz, averaged over three samples, were selected to allow a comparison between different materials (Table 2). For the emulsions with liquid paraffin G″ clearly dominated G′, indicating a more viscous than elastic behaviour. Interestingly, for the isopropyl myristate emulsions G′ and G″ were almost identical or they exhibited higher G′ than G″ values, indicating a more viscous fluid. Only IPM_3/37 showed behaviour comparable to that of the liquid paraffin emulsions; though, both values were notably low. The analysis of the tan δ values gave further insight into the viscoelastic properties of the formulations. Tan δ values > 1 indicate prevailing viscous behaviour, while values < 1 are characteristic for elastic systems [23,25]. While the liquid paraffin emulsions had tan δ values that were clearly above one, demonstrating that their behaviour was liquid-like; the isopropyl myristate emulsions showed values around 1.

Additional to visual and microscopic monitoring, the storage stability of the systems was investigated over a period of 20 weeks using rheological measurements. A large variation of the dynamic viscosity indicates changes in the inner structure of the formulation caused by phase separation or sedimentation. Thus, monitoring the rheological properties enables the detection of initial signs of instability before they become visible. Fig. 4 shows the dynamic viscosity of fresh and stored formulations compared at a shear rate of 10 s^{-1}. Overall, the emulsions revealed no statistical significant changes in the viscosity over the testing time with p values between 0.07 and 0.49, indicating a satisfying stability. In case of PAR_2/18, a significant increase in viscosity was observed after 20 weeks (p = 0.02) which may be a sign for changes in the inner structure of the formulation. However, the visual and microscopic appearance of PAR_2/18 did not imply any phase separations or changes.

3.3. Solubility study

For most diffusion studies, PBS is the receptor medium of choice. In

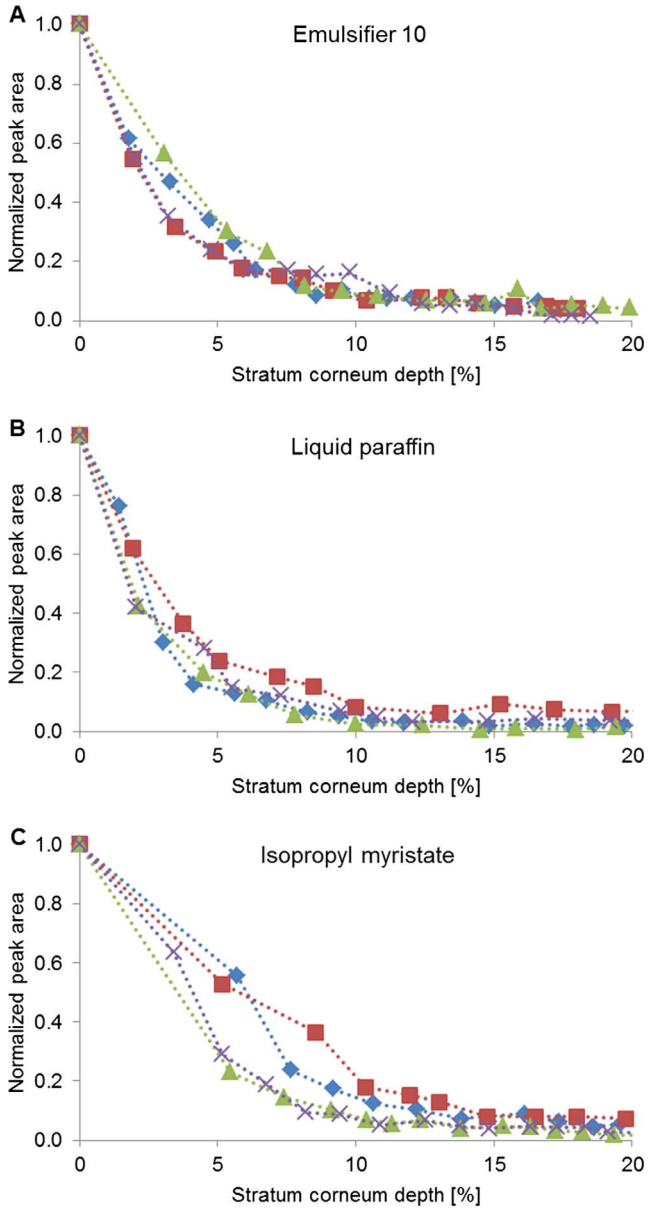

Fig. 7. Normalised characteristic absorbances of (A) Emulsifier 10, (B) liquid paraffin and (C) isopropyl myristate as a function of stratum corneum depth. To account for variability of contact between the ATR crystal and the skin, peak areas were related to the amide II absorbance. Different absorption coefficients were compensated by relating the absorbances to the corresponding absorbances of the respective reference spectra. The value 1 corresponds to the intensity ratio of the normalised absorbances from ATR-FTIR spectra recorded at the skin surface. Each curve respresents one experiment.

general, the concentration of permeant in the receptor medium should be kept below 10% of the saturation solubility to ensure sink conditions [26]. In the case of the highly lipophilic model drug curcumin, the receptor medium needs alteration in order to fulfil this criterion. The solubility of curcumin in a mixture of ethanol: PBS (50:50 v/v) was determined and a satisfying saturation solubility of 0.069 ± 0.004 mg/ml was found.

3.4. Skin permeation studies

Two formulations, PAR_2/18 and IPM_2/18, were chosen and loaded with model drugs in order to test their skin permeation. The hydrophilic fluorescein sodium and lipophilic curcumin served as model drugs.

The results of the *in vitro* skin permeation experiments for fluorescein sodium are shown in Fig. 5A. As can be seen, the skin permeation of fluorescein sodium from IPM_2/18 was considerably higher than from PAR_2/18. Statistical analysis yielded that the permeation of the model drug from IPM_2/18 was significantly higher at each time point compared to PAR_2/18 ($p < 0.001$). These findings indicate that the drug permeation is promoted by isopropyl myristate as the formulations are identical except for the oil compound. This is in line with existing literature, as isopropyl myristate has been suggested to promote drug solubility in the skin [27,28].

In case of curcumin, a trend to higher skin permeation from PAR_2/18 was observed (Fig.5B). In this respect, the overall very low permeation rates of the model drug should be taken into account. Although the high lipophilicity of curcumin was considered in the experimental setup, the permeated amounts were scarcely detectable. In addition, Fig.5B indicates that a considerable standard deviation is prevalent in the permeation data of curcumin.

3.5. Combined ATR-FTIR and tape stripping experiments

It was of interest to determine the penetration depth of the silicone surfactant in order to gain information about its behaviour on skin. Silicones are considered to be safe for topical use as they are non-toxic and do not interact with the microstructure of SC lipids [3,6]. Presumably, skin irritation is linked to the spatial distribution of a surfactant in the SC [9]. Thus, combined ATR-FTIR and tape stripping experiments were conducted to investigate the skin penetration of the deployed surfactant Emulsifier 10.

Initially, a spectrum of the pure Emulsifier 10 was recorded to identify the most prominent bands. The three dominant peaks at 1257, 1094 and 1014 cm^{-1} could be assigned to the vibrational modes of silicones, namely the CH_3 symmetric deformation and the Si—O—Si stretching [29,30].

In Fig. 6A, a spectrum of porcine ear skin incubated with water is overlaid with a spectrum of porcine ear skin incubated with Emulsifier 10; the previously attributed silicone bands are clearly visible. Fig. 6B shows the difference spectra from the tape-stripped layers that were obtained by subtracting the corresponding spectra of the water incubated control samples from the treated samples. As can be seen, the remaining absorbance matches with the characteristic absorption bands of the reference spectrum of the pure silicone surfactant. As the skin is sequentially removed with the tapes, absorbance decreases steadily. For the analysis of the penetration of the silicone surfactant into the skin tissue, the spectral ranges of (^{*1}) 1272–1245 cm^{-1} and ($^*2 + {}^*3$) 1130–988 cm^{-1} assigned to the vibrational modes of the Si—CH_3 bond and the Si—O—Si bond were selected for integration [30]. Subsequently, the thereby calculated absorbance was summed up. The accuracy of this method depends on the linear relationship of the two defined integration areas. To make sure that this is the case for the applied method, the depth-dependent absorbance of the two defined areas was correlated with each other. A correlation coefficient of 0.999 demonstrated the accuracy of the developed method.

The intensities of the integrated absorption areas were further processed by relating them to the respective amide II absorbance as well as to the absorbance of the reference spectrum of the emulsifier in direct contact with the ZnSe crystal. In Fig.7A, the summed up normalised absorbance was plotted against the SC depth calculated from the amount of corneocytes removed. A rapid decrease of the silicone surfactant concentration with skin depth was observed; it was traceable until about 15% of the SC depth. As reported in the literature, there might be a direct relation between the spatial distribution of a substance in the SC and its effects on skin barrier function [9,31]. Hence, the limited transdermal penetration of the silicone component is in good agreement with its commonly known safety profile; it indicates low irritation potency.

Additional to the determination of Emulsifier 10 in the SC, the oil components liquid paraffin and isopropyl myristate were investigated

by ATR-FTIR spectroscopy in the same manner. In short, characteristic vibrational modes were determined by recording spectra of the pure substances and integration ranges were defined. The frequency limits were 1478–1430 cm^{-1} and 1385–1363 cm^{-1} for liquid paraffin, 1761–1718 cm^{-1} and 1124–1093 cm^{-1} for isopropyl myristate. Fig. 7B and C show the calculated relative concentrations of both oils as a function of SC depth. Similar to the silicone surfactant, both oils were only detectable in the outermost area of the SC, with a more rapid decline of the amounts of incorporated liquid paraffin with increasing strip number. The results correspond with findings reported in literature [32–34]. By means of various techniques, a penetration of several oils into deeper layers of the stratum could not be detected.

4. Conclusion

Novel W/O emulsions stabilised by a silicone surfactant were successfully formulated. They exhibited an excellent stability and intriguing skin feel; this is attributed to the emulsion type and the outstanding physical properties of the emulsifier. Variation of the formulation composition revealed that the nature of the oil phase and the proportion of the ingredients have a strong impact on the microstructure and properties of the emulsion. Rheological measurements showed a strong dependency of viscosity on the water content. Hence, these novel emulsions offer the possibility to adjust their viscosity to individual requirements.

In vitro studies showed a significant influence of the deployed oil on drug delivery into the skin; an enhanced permeation of the hydrophilic model drug from the emulsion formulated with isopropyl myristate could be demonstrated. Advantageously, additive constituents, which may have undesired effects on the skin, hardly penetrated the outermost layers of the SC.

Based on these results, the formulations developed in the present study can be considered as potential novel conveniently applicable drug delivery options. Thanks to their unique properties, they are ideally suited for both pharmaceutical and cosmetic applications.

Acknowledgements

This work was financed by the Austrian Science Fund (FWF): P24846-B20 granted to Prof. Dr. Claudia Valenta and by the research platform “Characterisation of Drug Delivery Systems on Skin and Investigations of Involved Mechanisms”, University of Vienna.

References

[1] D.T. Floyd, Silicone surfactants: applications in personals care industry, in: R.M. Hill (Ed.), Silicone Surfactants, Marcel Dekker Inc., New York, 1999, pp. 181–209.
[2] P. Somasundaran, S.C. Mehta, P. Purohit, Silicone emulsions, Adv. Colloid Interface Sci. 128–130 (2006) 103–109, http://dx.doi.org/10.1016/j.cis.2006.11.023.
[3] B. Glombitza, C.C. Müller-Goymann, Investigation of interactions between silicones and stratum corneum lipids, Int. J. Cosmet. Sci. 23 (2001) 25–34, http://dx.doi.org/10.1046/j.1467-2494.2001.00054.x.
[4] K. De Paepe, A. Sieg, M. Le Meur, V. Rogiers, Silicones as nonocclusive topical agents, Skin Pharmacol. Physiol. 27 (2014) 164–171.
[5] M. Roberts, Y. Mohammed, M. Pastore, S. Namjoshi, S. Yousef, A. Alinaghi, I. Haridass, E. Abd, V. Leite-Silva, H. Benson, J. Grice, Topical and cutaneous delivery using nanosystems, J. Control. Release. 247 (2016) 86–105, http://dx.doi.org/10.1016/j.jconrel.2016.12.022.
[6] J. Lewandowska-Łańcucka, K. Mystek, A. Gilarska, K. Kamiński, M. Romek, B. Sulikowski, M. Nowakowska, Silicone-stabilized liposomes as a possible novel nanostructural drug carrier, Colloids Surf. B Biointerfaces 143 (2016) 359–370, http://dx.doi.org/10.1016/j.colsurfb.2016.03.057.
[7] M. Branagan, D.H. Chenery, S. Nichelson, Use of infrared attenuated total reflectance spectroscopy for the in vivo measurement of hydration level and silicone distribution in the stratum corneum following skin coverage by polymeric dressings, Ski. Pharmacol Appl Ski. Physiol. 13 (2000) 157–164.
[8] H.M. Klimisch, G. Chandra, Use of Fourier transform infrared spectroscopy with attenuated total reflectance for in vivo quantitation of polydimethylsiloxanes on human skin, J. Cosmet. Sci. 37 (1986) 73–87.
[9] G. Mao, C.R. Flach, R. Mendelsohn, R.M. Walters, Imaging the distribution of sodium dodecyl sulfate in skin by confocal Raman and infrared microspectroscopy, Pharm. Res. 29 (2012) 2189–2201, http://dx.doi.org/10.1007/s11095-012-0748-y.
[10] F.P. Schmook, J.G. Meingassner, A. Billich, Comparison of human skin or epidermis models with human and animal skin in in-vitro percutaneous absorption, 215 (2001) 51–56.
[11] U. Jacobi, M. Kaiser, R. Toll, S. Mangelsdorf, H. Audring, N. Otberg, Porcine ear skin: an in vitro model for human skin, 2007, pp. 19–24. 10.1111/j.1600-0846.2006.00179.x.
[12] C.H. Liu, F.Y. Chang, D.K. Hung, Terpene microemulsions for transdermal curcumin delivery: effects of terpenes and cosurfactants, Colloids Surf. B Biointerfaces 82 (2011) 63–70, http://dx.doi.org/10.1016/j.colsurfb.2010.08.018.
[13] M. Hoppel, D. Baurecht, E. Holper, D. Mahrhauser, C. Valenta, Validation of the combined ATR-FTIR/tape stripping technique for monitoring the distribution of surfactants in the stratum corneum, Int. J. Pharm. 472 (2014) 88–93, http://dx.doi.org/10.1016/j.ijpharm.2014.06.011.
[14] F. Spies, E. Boelsma, A.M. Mommaas, H.K. Koerten, Tape stripping of human stratum corneum yields cell layers that originate from various depths because of furrows in the skin, 1997, pp. 514–518.
[15] D.S. Mahrhauser, C. Nagelreiter, S. Gehrig, A. Geyer, M. Ogris, K. Kwizda, C. Valenta, Assessment of Raman spectroscopy as a fast and non-invasive method for total stratum corneum thickness determination of pig skin, Int. J. Pharm. 495 (2015) 482–484, http://dx.doi.org/10.1016/j.ijpharm.2015.09.018.
[16] T.M. Greve, K.B. Andersen, O.F. Nielsen, ATR-FTIR, FT-NIR and near-FT-Raman spectroscopic studies of molecular composition in human skin in vivo and pig ear skin in vitro, Spectroscopy. 22 (2008) 437–457, http://dx.doi.org/10.3233/SPE-2008-0365.
[17] V. Klang, M. Hoppel, C. Valenta, Infrared Densitometry for In Vitro Tape Stripping: Quantification of Porcine Corneocytes, in: P. Humbert, H. Maibach, F. Fanian, P. Agache (Eds.), Meas. Ski. Springer International Publishing, Cham, 2016, pp. 1–8, , http://dx.doi.org/10.1007/978-3-319-26594-0_27-1.
[18] L. Franzen, M. Windbergs, S. Hansen, Assessment of near-infrared densitometry for in situ determination of the total stratum corneum thickness on pig skin: influence of storage time, Skin Pharmacol. Physiol. 25 (2012) 249–256, http://dx.doi.org/10.1159/000339905.
[19] V. Klang, J.C. Schwarz, N. Matsko, E. Rezvani, N. El-Hagin, M. Wirth, C. Valenta, Semi-solid sucrose stearate-based emulsions as dermal drug delivery systems, Pharmaceutics. 3 (2011) 275–306, http://dx.doi.org/10.3390/pharmaceutics3020275.
[20] H. Lambers, S. Piessens, A. Bloem, H. Pronk, P. Finkel, Natural skin surface pH is on average below 5, which is beneficial for its resident flora, Int. J. Cosmet. Sci. 28 (2006) 359–370, http://dx.doi.org/10.1111/j.1467-2494.2006.00344.x.
[21] S.R. Derkach, Rheology of emulsions, Adv. Colloid Interface Sci. 151 (2009) 1–23, http://dx.doi.org/10.1016/j.cis.2009.07.001.
[22] J.-L. Salager, Emulsion Properties and Related Know-how to Attain Them, Pharm. Emuls. Suspens. Second ed. Revis. Expand. CRC Press, 2000, pp. 73–125, , http://dx.doi.org/10.1201/b14005-4.
[23] M. Gašperlin, L. Tušar, M. Tušar, J. Kristl, J. Šmid-Korbar, Lipophilic semisolid emulsion systems: viscoelastic behaviour and prediction of physical stability by neural network modelling, Int. J. Pharm. 168 (1998) 243–254, http://dx.doi.org/10.1016/S0378-5173(98)00099-4.
[24] C. Valenta, C.E. Kast, I. Harich, A. Bernkop-Schnürch, Development and in vitro evaluation of a mucoadhesive vaginal delivery system for progesterone, J. Control. Release. 77 (2001) 323–332, http://dx.doi.org/10.1016/S0168-3659(01)00520-X.
[25] R.G. Riley, J.D. Smart, J. Tsibouklis, P.W. Dettmar, F. Hampson, J.A. Davis, G. Kelly, W.R. Wilber, An investigation of mucus/polymer rheological synergism using synthesised and characterised poly(acrylic acid)s, Int. J. Pharm. 217 (2001) 87–100, http://dx.doi.org/10.1016/S0378-5173(01)00592-0.
[26] K.R. Brain, K.A. Walters, A.C. Watkinson, Investigation of skin permeation in vitro, in: M.S. Roberts, K.A. Walters (Eds.), Dermal Absorpt. Toxic. Assess. Marcel Dekker Inc., New York, 1998, pp. 161–187.
[27] P. Santos, A.C. Watkinson, J. Hadgraft, M.E. Lane, Influence of penetration enhancer on drug permeation from volatile formulations, Int. J. Pharm. 439 (2012) 260–268, http://dx.doi.org/10.1016/j.ijpharm.2012.09.031.
[28] M.E. Lane, Skin penetration enhancers, Int. J. Pharm. 447 (2013) 12–21, http://dx.doi.org/10.1016/j.ijpharm.2013.02.040.
[29] I. Noda, A.E. Dowrey, J.L. Haynes, C. Marcott, Group Frequency Assignments for Major Infrared Bands Observed in Common Synthetic Polymers, Phys. Prop. Polym. Handb. Springer, New York, 2007, pp. 395–406, , http://dx.doi.org/10.1007/978-0-387-69002-5_22.
[30] A. Lanzarotta, C.M. Kelley, Forensic analysis of human autopsy tissue for the presence of polydimethylsiloxane (silicone) and volatile cyclic siloxanes using macro FT-IR, FT-IR spectroscopic imaging and headspace GC-MS, J. Forensic Sci. 61 (2016) 867–874, http://dx.doi.org/10.1111/1556-4029.13018.
[31] M.C. Mack Correa, G. Mao, P. Saad, C.R. Flach, R. Mendelsohn, R.M. Walters, Molecular interactions of plant oil components with stratum corneum lipids correlate with clinical measures of skin barrier function, Exp. Dermatol. 23 (2014) 39–44, http://dx.doi.org/10.1111/exd.12296.
[32] C. Choe, J. Lademann, M.E. Darvin, Analysis of human and porcine skin in vivo/ex vivo for penetration of selected oils by confocal Raman microscopy, Skin Pharmacol. Physiol. 28 (2015) 318–330, http://dx.doi.org/10.1159/000439407.
[33] A. Patzelt, J. Lademann, H. Richter, M.E. Darvin, S. Schanzer, G. Thiede, W. Sterry, T. Vergou, M. Hauser, In vivo investigations on the penetration of various oils and their influence on the skin barrier, Ski. Res. Technol. 18 (2012) 364–369, http://dx.doi.org/10.1111/j.1600-0846.2011.00578.x.
[34] G.N. Stamatas, J. de Sterke, M. Hauser, O. von Stetten, A. van der Pol, Lipid uptake and skin occlusion following topical application of oils on adult and infant skin, J. Dermatol. Sci. 50 (2008) 135–142, http://dx.doi.org/10.1016/j.jdermsci.2007.11.006.